Multi-scale homogeneity analysis of co-milled powders : development of a reverse approach to assess quality of mixtures

Martin Giraud, Cendrine Gatumel, Stéphane Vaudez, Jeremy Nos, Thierry Gervais, Guillaume Bernard-Granger, Henri Berthiaux

Title:
Multi-scale homogeneity analysis of co-milled powders : development of a reverse approach to assess quality of mixtures

Authors:

Martin GIRAUD[a,b], Cendrine GATUMEL[a], Stéphane VAUDEZ[b], Jeremy NOS[c], Thierry GERVAIS[d], Guillaume BERNARD-GRANGER[b], Henri BERTHIAUX[a]

[a] Laboratoire RAPSODEE, UMR CNRS 5302, IMT Mines Albi, Campus Jarlard, 81013 Albi Cedex 09, France
[b] CEA, DEN, ISEC, DMRC, Université de Montpellier, Marcoule, France
[c] Orano, 125 avenue de Paris, 92320 Châtillon, France
[d] Orano Melox, Les Tourettes, D138A, 30200 Chusclan, France

Corresponding author:

Henri BERTHIAUX[a] – henri.berthiaux@mines-albi.fr

Abstract:

The standard methodology employed for estimating homogeneity of powder mixtures relies on the concept of scale of scrutiny. This parameter defines the relevant scale at which a homogeneous distribution of a given compound is critical regarding the final application of the blend. However, such a scale is not always known in advance. In this paper, a process involving two ceramic powders, co-ground and pressed into pellets is investigated in terms of homogeneity at various scales, from macroscopic to microstructural. According to the scale considered, different methodologies are employed. In particular, a reverse method is developed providing homogeneity indexes that are characterizing the microstructural state, without knowing the scale of scrutiny in advance. The results show that the homogeneity is improved by the co-grinding process as compared to simple drum-mixing experiments, even at a macroscopic scale. This method also shows that the microstructural homogeneity increases according to the grinding time during the first 16 minutes of grinding.

The evolution of the microstructural homogeneity according to the grinding time is also investigated.

Keywords:

Powder mixture – ball milling – homogenization – MSAAF

Nomenclature:

Notation	Parameter	Usual units
C	Concentration	g.ml^{-1}
CV	Coefficient of variation	-
$\bar{d}$	Mean particle diameter (on SEM images)	µm
d_S	Average diameter of the surface particle size distribution	µm
H_i	Homogeneity index relative to a CV of i %	-
J	Pebbles filling ratio	-
n	Number of particles in a given sample	-
$\bar{n}$	Average number of particle in a given cell	-
$p(n_i)$	Probability of obtaining n_i particles in a given cell	-
Q	Cell size	Pixels or mm
q	Cell depth	µm
t	Grinding time	min
t_S	Student parameter	-
U	Level of powder	-
V_i	Volume of the element i	ml
w	Mass fraction of alumina	-
W_i	Mass of a sample providing a CV of i %	µg
z	Surface fraction of alumina	
Greek letters		
ε_g	Pebbles bed porosity	-
η_{Al/Al_2O_3}	Mass of aluminum atoms in alumina	-
η_{Zr/ZrO_2}	Mass of zirconium atoms in zirconia	-
λ	Dimensionless cell size	-
$\bar{\mu}$	Average composition measured	-
Ω	Rotational speed of the vessel	rpm
ρ_{pellet}	Apparent density of a pellet	g.ml^{-1}
ρ_s	True density	g.ml^{-1}
ς	Standard deviation of the composition measured	-
ς^2	Variance of the composition measured	-
Frequently used indexes		
0	Relative to a segregated mixture	
BSE	Measured by BSE	
cha	Relative to the characterization method	
EDS	Measured by EDS	
ICP	Measured by ICP	
mes	Measured	
mix	Relative to the mixture	
r	Relative to a random mixture	
sam	Relative to the sampling protocol	
ρ	Measured by helium pycnometry	

Abbreviations:

CV: Coefficient of variation

DVS: Dynamic Vapor Sorption

EDS: Energy Dispersive X-ray Spectroscopy

ICP-AES: Inductively Coupled Plasma Atomic Emission Spectroscopy

SEM: Scanning Electron Microscopy

WD: Working Distance

1. Introduction

Most granular media involved in industrial processes are actually composed of several ingredients, as for examples Active Pharmaceutical Ingredients (API) and excipients for drug preparation or various pigments for inks and paints manufacturing. In such powder mixtures, homogeneity is the most critical parameter that defines the quality of the final product. Indeed, the distribution of the ingredients within the blend can influence its main properties, such as its taste, its color and its bio-availability for example. For solid materials that are manufactured from powders by sintering, molding or extrusion, the homogeneity of the initial powder blend can have an impact on the material's key properties such as its mechanical strength or its electrical conductivity, for instance.

As highlighted by Harnby, the concept of homogeneity can only be relevant when it is associated to a given scale, named the scale of scrutiny (Harnby, 1992). For example, in the case of pharmaceutical tablets manufacturing, the API is expected to be distributed evenly over the pills manufactured. Thus, the relevant scale of scrutiny corresponds to the size of a tablet and the powder preparation does not need to be homogenous at a much smaller scale. However, if those tablets are divisible, the scale of scrutiny should then be adjusted to the size of the smallest fragment disposable (Berthiaux, 2002). Accordingly, the homogeneity of a given powder mixture is directly related to its future usage. The scale of scrutiny then corresponds to the relevant scale at which the homogeneity of the blend must be investigated in order to control its quality for a given application.

Danckwerts suggested a method for quantifying the homogeneity of a given mixture, involving two virtually independent quantities: the scale and the intensity of segregation (Danckwerts, 1952). The scale of segregation is representative of the structure of the powder blend, which is an intrinsic property of the mixture. It can be estimated from auto-correlation functions that characterize the state of subdivision of the particulate system (Danckwerts, 1953). On the other hand, the intensity of segregation corresponds to the variations among the sample's composition and can be determined with various mixing indexes derived from the standard deviation, ς, between the sample's compositions (Lacey, 1954). Thereby, the scale of scrutiny must be known in advance in order to define the sample size. Knowing the scale of scrutiny, the sampling procedure can be determined by defining the number of samples, their size, their location within the blend and the technique employed for extracting the samples. Then, each sample is characterized in order to determine its composition. The choice of the characterization method is a critical issue for the estimation of the homogeneity; this will be discussed in further details in the next paragraph. Finally, the scale and the intensity of segregation can be assessed from the variance between each sample's compositions. The variance obtained, ${\varsigma_{\mathrm{mes}}}^2$, is actually the sum of all variances resulting from the sampling procedure, the characterization method and the mixing step, as shown in equation (1) (Poux et al., 1991).

$$ {\varsigma_{\mathrm{mes}}}^2 = {\varsigma_{\mathrm{sam}}}^2 + {\varsigma_{\mathrm{cha}}}^2 + {\varsigma_{\mathrm{mix}}}^2 \quad (1) $$

In this equation, ${\varsigma_{\mathrm{mix}}}^2$ is the actual variance of the mixture related to its homogeneity. This means that the sampling procedure and the characterization method should be determined in order to minimize the corresponding variances ${\varsigma_{\mathrm{sam}}}^2$ and ${\varsigma_{\mathrm{cha}}}^2$, respectively.

In practice, the intensity of segregation is usually represented by the coefficient of variation, CV, defined by equation (2) as the ratio between the standard deviation, ς, and the average, $\bar{\mu}$.

$$ CV = \frac{\varsigma}{\bar{\mu}} \quad (2) $$

The variance attributed to the sampling procedure is of statistical order and can be reduced by increasing the amount of samples, selecting the sample's location randomly and choosing a sampling method that does not perturb too much the powder structure. The variance corresponding to the characterization method is related to the technical considerations depending on the method itself. The characterization

method should be selected in accordance with the elementary powders constituting the blend. For example, Massol-Chaudeur had to compare various techniques such as ultraviolet-visible spectrometry, colorimetric titration, differential scanning calorimetry, and high performance liquid chromatography in terms of selectivity, linearity, exactitude, sensitivity and reproducibility in order to be able to select which one is the most adequate for assessing the homogeneity of a mixture containing 99 wt% of lactose and 1 wt% of sodium saccharin (Massol-Chaudeur, 2000). Furthermore, the characterization technique must allow the measurement of samples whose size is equal to the scale of scrutiny.

It appears that, using such a methodology, the scale of scrutiny is a critical parameter since it defines the sampling procedure and adds a significant constraint for selecting the best characterization method. However, in many cases where the link between the powder blend structure and its final properties is not known, such a scale is not clearly defined. In particular, this is the case for powder mixtures that are meant to be transformed, by pressing or molding, before usage. For instance, Mayer-Laigle investigated the homogeneity of powder mixtures made of graphite and epoxy resin, that are then molded and thermoset in order to make bipolar plates used in fuel cells stacks (Mayer-Laigle et al., 2011). In this example, the presence of segregated area in the initial powder blend leads to small residual defects in the final plates. These affect the plate's mechanical properties and may cause their rupture during the demolding step. The link between the powder mixture quality, the size, the number of defects present at the surface of the plates and their mechanical properties is not clearly established. Thus, the lack of scale of scrutiny makes the definition of an adequate acceptability criteria very difficult, as highlighted by the author (Mayer-Laigle et al., 2011). In such cases, the homogeneity should be assessed at various scales of scrutiny, in order to provide the evolution of the variance of the mixture according to the scale considered. In order to address this issue, Buslik proposed a definition for a homogeneity index, H_1, defined by equation (3), that is based on the parameter W_1 which corresponds to the weight of a sample required to obtain a coefficient of variation of 1% (Buslik, 1973).

$$H_1 = \log\frac{1}{W_1} = -\log W_1 \qquad (3)$$

Such a method can be seen as a "reverse method", as compared to the standard one. Indeed, in this method, an acceptable intensity of segregation is first of all defined, 1% for Buslik, and then the scale which ensures such mixture quality is determined. One of the main advantages of this approach is that it does not require the knowledge of the relevant scale associated to the product's final usage, which, as mentioned in the previous paragraph, may be a problematic issue. Moreover, this approach makes a lot of sense in many industrial fields where the quality of the product is at first defined by a coefficient of variation. For example, in the pharmaceutical industry dealing with manufacturing pills from powder mixtures, a mandatory acceptability criterion is to obtain a coefficient of variation of the API distribution strictly below 6% (Bergum et al., 2014; FDA, 2003). Thus, the reverse method provides the minimal scale for which this restriction is valid. Finally, it can be argued that this method requires sampling and analyzing the mixture at various scales, which increases considerably the complexity of the experimental protocol. However, for many characterization methods, in particular those based on image analysis, it should not be so difficult. For example, a picture obtained by scanning electron microscopy (SEM) at a small magnification can be easily fragmented into smaller parts whose sizes can be determined arbitrarily.

In this paper, we will focus on a given process used for the preparation of ceramic pellets from a powder mixture prepared by co-grinding in a ball mill (see Figure 1). The first step of this process consists in mixing the powders together in the ball mill. In such an operation, the homogenization of the mixture takes place simultaneously with the fragmentation of the agglomerates constituting the raw powders. As compared with a simple drum mixer, the ball mill process should provide a better homogenization by decreasing the particle's size and thus increasing the number of particles at a given scale. Indeed, the minimal achievable variance for a given powder increases with the number of elementary particles. This

a suppri

can be illustrated by the definition of the variance of a random binary mixture, ς_r^2, given by equation (4), where w is the global mass composition of the mixture and n is the number of particles in a sample (Lacey, 1954).

$$\varsigma_r^2 = \frac{w(1-w)}{n} \tag{4}$$

The last two steps of the process consist in shaping cylindrical pellets of approximately one gram by uniaxial-pressing at room temperature and consolidating the pellets by sintering in an oven using an optimum thermal treatment. In this study, we will focus only on the homogeneity of the green pellets obtained before sintering, since the homogeneity of the pellets is not expected to vary that much after sintering because the selected powders do not react whith each other to form an additional phase during the thermal treatment retained. In this case, various degrees of homogeneity can be defined to characterize the quality of the green product. First, we can consider the "macro-homogeneity" for which the scale of scrutiny is defined as the size of a pellet (one gram). The macro-homogeneity characterizes the probability of getting the same composition among the pellets manufactured. A second degree of homogeneity, the "microstructural homogeneity", corresponds to a much finer scale, inside a given pellet and is related to its behavior regarding the manufactured product's final application. The scale of scrutiny for this microstructural homogeneity is not clearly defined since it depends on the requirements linked to the pellet's usage. Moreover, the microstructural homogeneity at a given scale is expected to vary according to the co-grinding conditions. Indeed, the number, n, of particles in a sample is expected to increase during the grinding operation, which leads potentially to a higher homogeneity at a given scale, as shown in equation (4). Conversely, a smaller size of scrutiny is expected to provide a higher intensity of segregation. Both types of homogeneity under investigation are summarized in Table 1.

a suppri

Table 1: Different types of homogeneity under investigation.

Type of homogeneity	Scale
Macro-homogeneity	One pellet ($1\ g$)
Microstructural homogeneity	Variable (approximately $1\ \mu g\ -1\ mg$)

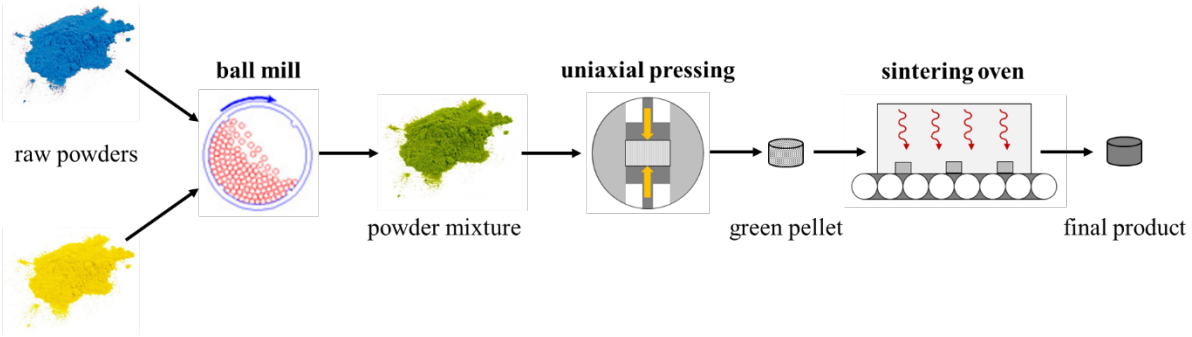

Figure 1: Schematic representation of the process investigated in this study.

The methodology presented in this introduction will be employed in order to estimate the homogeneity of the pellets at the macroscopic scale, for various ball milling conditions. Then, a methodology involving the reverse approach will be investigated in order to provide an estimation of the green pellets microstructural homogeneity scale.

2. Materials and methods

2.1. Pellets preparation

2.1.1.Powders

The powder mixtures prepared for this work are composed of two raw ceramic powders : a zirconia (ZrO_2) GY3Z-R60 powder from Saint Gobain® (Courbevoie, France) and an alumina GE15 powder from Baikowski® (Poisy, France). Both volume particle size distributions corresponding to these raw powders are shown on Figure 2. They have been measured by LASER diffraction with a Mastersizer® 3000 equipment (Malvern, Malvern, UK), using the liquid dispersion unit Hydro MV® operating with water. It appears that the alumina powder exhibits a higher fraction of fine particles as compared to the zirconia one, in particular in the range below 20 μm. On the other hand, the zirconia powder is made of bigger particles, some being much larger than 100 μm. Some typical particles constituting both powders are shown on Figure 3, the pictures have been acquired using an ESEM-FEG XL30® (Philips, Amsterdam, Nederland) in secondary electron mode. The zirconia particles are quite spherical while the alumina ones are more angular and exhibit a tablet shape. Previous investigations carried out with these powders, using shear tests, showed that the GE15 alumina powder flows poorly as compared to the GY3Z-R60 zirconia one, which exhibits a free flowing behavior (Giraud et al., 2020). Obviously, the particle's size and shape as well as the flowability of these powders are expected to vary significantly during the grinding operation.

a suppri

a suppri

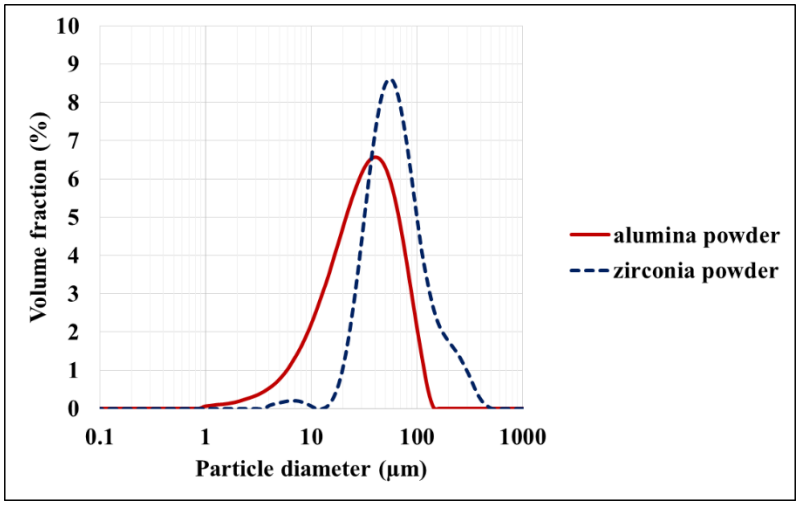

Figure 2: Volume particle size distribution of both raw powders.

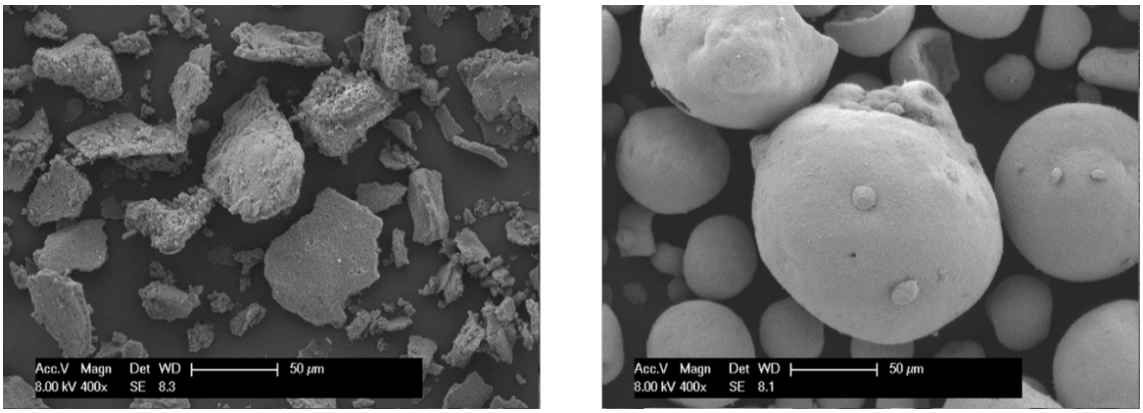

Figure 3: SEM pictures obtained for the alumina (left) and the zirconia (right) powders.

2.1.2. Ball milling

The ball mill is constituted of a 1 l cylindrical vessel made of stainless steel, filled with a given amount of pebbles that are used as grinding media, as shown on the picture located on the right side of Figure 4. The pebbles are steel cylinders of dimensions (diameter and height) $8 \times 8\,mm$. The number of pebbles introduced into the vessel is set to 500, ensuring a pebble's filling ratio of $J = 0.3$, where J is defined by equation (5):

$$J = \frac{V_{\text{pebbles}}}{V_{\text{vessel}}} \tag{5}$$

where V_{vessel} is the inner volume of the vessel and V_{pebbles} is the apparent volume of the pebbles bed.

The powders are poured into the vessel in order to obtain a powder level of $U = 1.0$, meaning that the powder arises at the same level than the pebbles bed when the vessel is at rest. The powder level, U, is defined by equation (6):

$$U = \frac{V_{\text{powder}}}{\varepsilon_g \cdot V_{\text{pebbles}}} \tag{6}$$

where V_{powder} is the apparent volume of the powder bed poured into the vessel and $\varepsilon_g = 0.33$ is the porosity of the bed. It was measured by filling the vessel with water and estimating the volume needed to fill the porosities between the pebbles.

The amount of zirconia and alumina powders are defined in order to obtain a mass fraction of alumina $w = 0.30$. The vessel is filled vertically, the pebbles are introduced first and the powders are then poured one after the other, starting with the less flowable one, the alumina powder.

Finally, as shown on Figure 4, the vessel rotates around its longitudinal axis, at a given rotational speed, Ω, that is measured with a tachometer DT-2236® (Lutron electronic, Taipei, Taiwan). In order to investigate the influence of the grinding conditions on the homogeneity of the resulting powder mixtures, four grinding test, denoted as B01, B02, B03 and B12 were performed with various rotational speeds and for various grinding times. The grinding conditions corresponding to each test are summarized in Table 2. A powder mixture, M01, was prepared in a Turbula T2F® mixer in order to compare the results obtained by co-grinding with the one obtained using a single drum mixer. The M01 blend was prepared in a 300 ml polyethylene vessel, filled with powder to 40% of its maximum capacity. The Turbula rotational speed was set to 32 rpm for 10 minutes. Such mixing conditions were shown to ensure a good homogeneity for similar powder mixtures (Mayer-Laigle et al., 2015).

Table 2: Mass fraction of alumina, w, rotational speed, Ω, and grinding time, t, corresponding to each mixing/grinding tests.

Test name	Equipment	w	Ω (rpm)	t (min)
M01	Turbula mixer	0.30	-	-
B01	Ball mill	0.30	25	1
B02	Ball mill	0.30	25	4
B03	Ball mill	0.30	25	8
B12	Ball mill	0.30	50	2

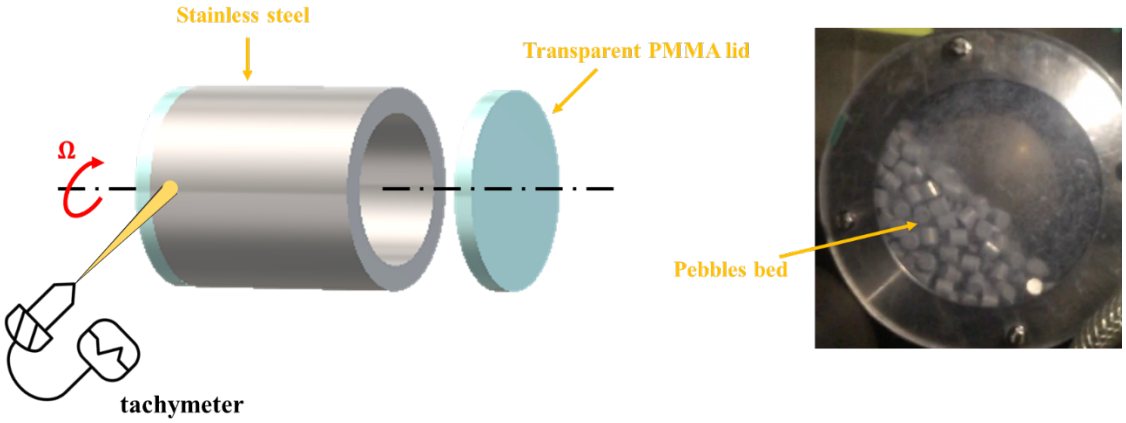

Figure 4: Schematic representation of the ball milling operation and picture taken from the rotating vessel with pebbles and without powder filling

2.1.3. Uniaxial-pressing

After each ball milling operation, the ground powders were spread out, as shown on Figure 5, and three samples of one gram each were randomly selected per test (including the M01 one). At first, the exact true density of each powder sample was measured (see section 2.2.1 for more details). Then, each powder sample was compacted with a uniaxial-press Instron 5567® (Instron, Elancourt, France). The obtained pellets, shown on Figure 5, are cylinders of diameter equal to 11.20 mm, their height varies depending on the grinding conditions. A normal compaction pressure of 263 MPa was employed in order to get a relative density around 50%, meaning that the pellets contained 50% of residual porosity.

Figure 5: Ground powder spread out for the sampling procedure (left) and pellets obtained after compacting (right)

2.2. Characterization methods

In the context of an estimation of the homogeneity, an ideal characterization method must allow a measurement of the sample's alumina content. The two main constraints for selecting the method are the compatibility with the sample size and the ability to measure the alumina concentration. Since both zirconia and alumina powders are of the same color, as shown on Figure 5, they cannot be differentiated from simple pictures by image analysis. The thermic methods can also be excluded due to the high temperature resistance of both materials. The two main characteristics that may differentiate both compounds are their true density and their atomic number. Accordingly, the two techniques used for measuring the alumina content in samples of various sizes are then described in the next paragraphs.

2.2.1. Helium pycnometry

A helium pycnometer AccuPyc II 1340® (Micromeritics, Mérignac, France) was used to measure the true density of the samples. A given sample is weighed and then introduced into a cell of a given volume, here 1 ml. Gaseous helium is then injected into the vessel containing the powder, at a given pressure of 135 kPa and under a temperature of 23 °C. Knowing precisely the cell's volume, the total volume

occupied by the powder sample can be deduced from the quantity of helium injected. Helium is chosen for its small atomic diameter, which ensured that the gas occupies the smallest cavities that may be present at the particles' surface. A cycle of measurement is composed of 25 purges, followed by 25 measurements, the average value being kept.

For each raw powder, five samples of 1 g were characterized, the average value was taken and the standard deviations were used as incertitude intervals. The measured true density was $\rho_{s,Al_2O_3} = 3.929 \pm 0.002\ \mathrm{g{\cdot}cm^{-3}}$ for the GE15 alumina powder and $\rho_{s,Zr_2O_2} = 5.354 \pm 0.002\ \mathrm{g{\cdot}cm^{-3}}$ for the GY3Z-R60 zirconia one. It appears possible to use these different values of true density in order to measure the alumina content incorporated in a given powder sample. For example, according to the values obtained for both raw powders, the true density of a sample containing exactly 30 wt% of alumina is expected to exhibit a true density of $\rho_{s,30\%} = 4.829 \pm 0.014\ \mathrm{g{\cdot}cm^{-3}}$, where the incertitude interval corresponds to the combined incertitude of both values obtained for the raw powders.

It should be also highlighted that no significant variations of the true density were measured after grinding both powders under various conditions. The same methodology can thus be applied to co-grinded powder mixtures of alumina and zirconia.

2.2.2. Scanning electron microscopy

A Quanta 200® ESEM FEG (FEI Company, Hillsboro, USA) was used for microscopic images acquisition of the green pellets microstructure. Since the pellets could not be split, the images were taken at their bottom surface. An electron beam is focused on the surface investigated, the interaction between the sample and the electrons produce various signals that can be analyzed by detectors. In particular, the amount of backscattered electrons (BSE) reaching the adequate detector is proportional to the atomic number of the element encountered by the primary electron beam. Thus, the regions of the samples containing mostly alumina will appear darker than the areas containing zirconia on the images acquired.

The SEM analyses were carried out without metalizing the pellets, with an acceleration voltage of 15 kV. The magnification was set to x80 at a working distance of 10.3 mm, providing images representing a surface of $1.8 \times 1.3\ mm^2$ with a resolution of 1.5 µm per pixel. One image was taken for each pellet, the obtained results are given on Figure 6 for each grinding condition.

a suppri

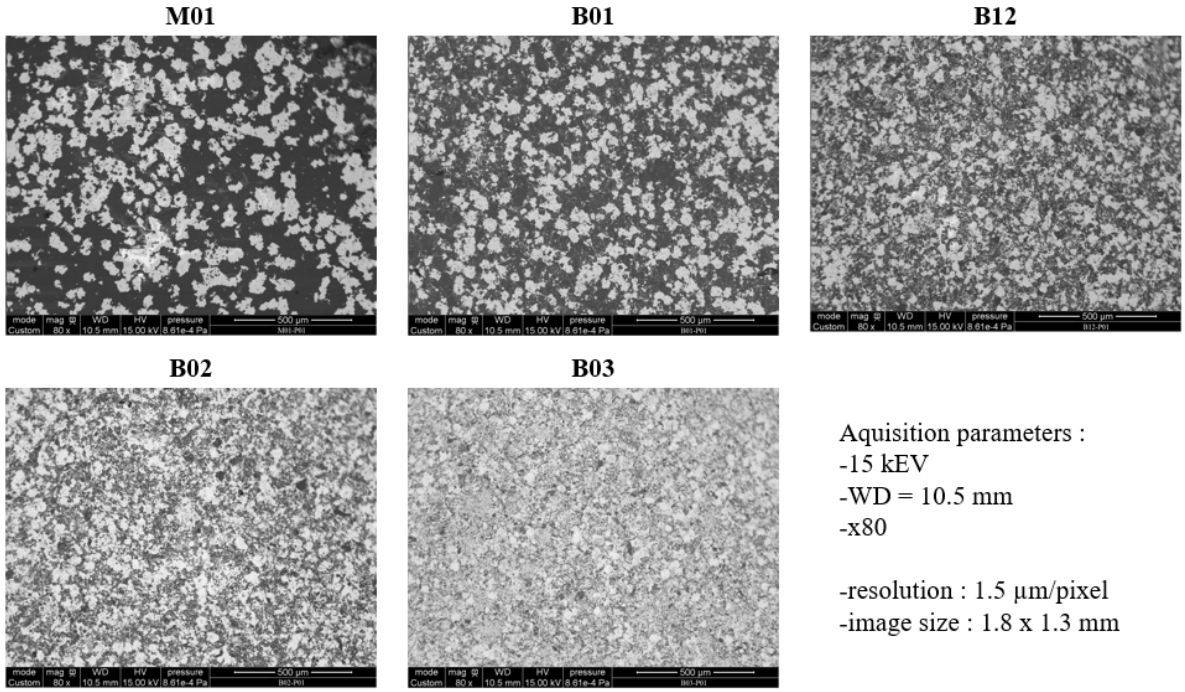

Figure 6: BSE-SEM images of the surface of pellets obtained in different grinding conditions (M01 is mixed without grinding, B01, B12; B02, B03 correspond to the various grinding conditions described in table 2)

The SEM device is also equipped with an X-ray detector allowing the energy-dispersive X-ray spectroscopy (EDS) analysis of investigated areas for a given sample. Accordingly, quantitative EDS maps of typical zones, as the ones shown on Figure 6, for the Al and Zr elements, have been performed using the Hypermap mode of the Esprit software (Bruker Nano GmbH, Berlin, Ge, standardless peak to background quantification method with ZAF correction, acceleration voltage set to 15 kV, Qmap resolution set to 1/2).

a suppri

3. Investigation of the macro-homogeneity

The stake of estimating the macro-homogeneity is to ensure that different pellets, coming from the same grinding test, share the same composition. Therefore, the scale of scrutiny in this case is 1 g, the mass of a given pellet.

3.1. Sampling protocol

For this protocol, the size of a sample is set to 1 g since the scale of scrutiny is clearly defined in this case. The total ground powder mass obtained after the ball milling step is around 70 g, with respect to the vessel size, the filling ratios and the mixture composition. The number of samples needed actually depends on the homogeneity of the mixture itself. Indeed, a very few amount of samples is needed to characterize a very homogeneous mixture while a larger amount is required if the composition varies widely among the samples. As a first approach, ten samples of one gram were considered, which represents approximately 14% of the whole ground powder batch under investigation. In order to get a random sampling, the whole ground mixture was spread out on a plastic strip, as shown on Figure 5, and divided into 40 compartments of equal sizes thanks to a measuring tape. All the compartments were indexed from 1 to 40 and 10 of them were randomly selected. Finally, a sample of one gram was randomly taken from each selected compartment.

a suppri

3.2. Characterization method: helium pycnometry

Helium pycnometry was retained for measuring the composition of the 1 g samples taken from the different ground powder mixtures. Indeed, the 1 ml cell of the AccuPyc II 1340® equipment is perfectly

adequate for characterizing samples of 1 g. As shown in section 2.2.1, the true density of a given sample can be used to determine its alumina content knowing the true density of both raw/ground powders taken individually (the grinding step was shown to have no influence on the true density of the alumina and zirconia powders). The mass fraction, w_{sample}, of alumina within the sample can be deduced from their true density thanks to equation (7).

$$w_{sample} = \frac{\rho_{s,Al_2O_3}\left(\rho_{s,sample} - \rho_{s,ZrO_2}\right)}{\rho_{s,sample}\left(\rho_{s,Al_2O_3} - \rho_{s,ZrO_2}\right)} \quad (7)$$

where $\rho_{s,sample}$ is the sample's measured true density and ρ_{s,Al_2O_3} and ρ_{s,ZrO_2} were measured in section 2.2.1.

Accordingly, the composition corresponding to each sample was measured for the M01, B01, B02 and B03 test conditions summarized in Table 3. In order to check the consistency of the methodology for poorly homogeneous mixtures, another blend, denoted as M00, has been carried out. The M00 mixture contained the same mass of powder and the same composition than the other mixtures but was prepared intentionally heterogeneous by shaking manually, for only a few seconds, a cylindrical vessel containing the powder without pebbles. Then, the same sampling and characterization methods were performed with this mixture.

3.3. Estimation of the macro-homogeneity

For each grinding test investigated, the average alumina contents, $\bar{\mu}_\rho$, measured among the ten samples are given in Table 3 with the corresponding standard deviations, ς_ρ. The coefficients of variation, CV_ρ are also calculated given in Table 3.

Table 3: Results obtained for the macro-homogeneity of the mixing and co-grinding tests.

Test	M00	M01	B01	B02	B03
$\bar{\mu}_\rho$	0.358	0.288	0.295	0.277	0.306
ς_ρ	0.183	0.009	0.005	0.005	0.005
CV_ρ	51.2%	3.12%	1.57%	1.98%	1.63%

At first, the M00 test exhibits a very high standard deviation of 0.183, as expected. This consistent result shows that the procedure employed for estimating the homogeneity seems to be valid for poorly mixed blends. As a comparison, this standard deviation is still significantly lower than the variance of the worst possible mixture, $\varsigma_0 = 0.458$ given by equation (8) (Lacey, 1954).

$$\varsigma_0 = \sqrt{w(1-w)} \quad (8)$$

Table 3 shows that the ground powder mixtures, B01, B02 and B03 exhibit a better homogeneity ($CV_\rho < 2\%$) than the simple powder mixture M01 ($CV_\rho = 3.12\%$) and that in all cases the average alumina weight content is close to the target one set to 0.30 for the experiments. This indicates that the ball milling operation seems to provide a better mixture at pellets' scale, as compared to the Turbula mixer regarding the experimental conditions used. This result is even more interesting considering the fact that all the grinding tests were performed for shorter grinding duration (1, 4 and 8 minutes for B01, B02 and B03, respectively) than the Turbula mixture (10 minutes for M01). This result does not necessarily comes from the grinder/mixer themselves but most probably from the increased number of particles in a given 1 g sample after grinding.

It should be noted that the standard deviations, given in Table 3, only account for the variability between the measurements carried out for different samples. Thus, they cannot be taken as an uncertainty value of the alumina content, which must be calculated by combining the standard deviations associated to the

values of ρ_{s,Al_2O_3} and ρ_{s,ZrO_2} that are involved in the composition calculation in equation (7). This may explain why the true mass fraction of the mixtures is not always included in the interval $[\bar{\mu}_\rho - \varsigma_\rho; \bar{\mu}_\rho + \varsigma_\rho]$, which does not represent a confidence interval.

Supposing that the standard deviations measured in Table 3 are close to the true standard deviations of the whole blends, we can estimate the number of samples needed for assessing the homogeneity as well as the confidence interval associated. Considering a normal distribution, the confidence interval associated to the average composition, $\bar{\mu}_\rho$, of a given blend and measured from a restricted number of samples, N, is given by equation (9).

$$I_c = \left[w - t_{S,1-\frac{\alpha}{2}}(N-1)\sqrt{\frac{\varsigma_\rho^2}{N}} \; ; \; w + t_{S,1-\frac{\alpha}{2}}(N-1)\sqrt{\frac{\varsigma_\rho^2}{N}} \right] \quad (9)$$

where $w = 0.30$ is the true composition of the blends and $t_{1-\frac{\alpha}{2}}(N-1)$ is the Student parameter associated to the risk α for a degree of freedom of $N-1$. This parameter can be found in a Student table.

The confidence intervals, given by the Student's law, for a risk $\alpha = 0.05$, are shown on Figure 7 for the blends M01 and B01. The dotted horizontal lines correspond to an interval of $\pm 2\%$ around the true composition w. For the B01 mixture, it appears that a number of 10 samples is more than enough for ensuring a valid composition, with a maximal error of 2%. However, the number of samples for the M01 mixture should be at least 12 to justify the same precision level.

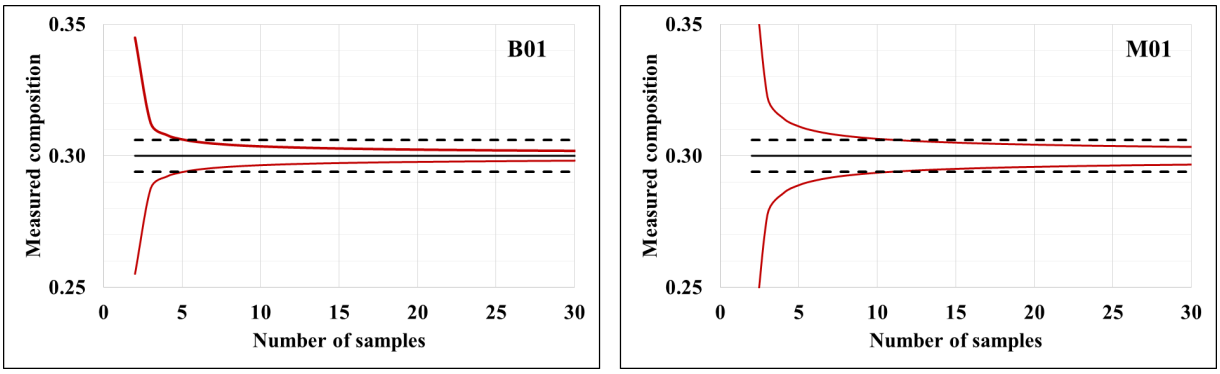

Figure 7: Confidence intervals given by the Student law for a risk of 0.05 according to the number of samples considered for the B01 and M01 tests.

As a conclusion to this section, we showed that the co-grinding process allowed a good macro-homogeneity at a pellet scale with a coefficient of variation below 2%. On the other hand, the standard mixing process, that do not involve grinding, gave a slightly higher coefficient of variation, around 3%, for the same mixture composition. However, it was not possible to compare two grinding conditions in terms of homogeneity at this scale of scrutiny: B01, B02 and B03 give very similar results. It can be considered that the variance attributed to the homogeneity of the mixture, ς^2_{mix}, at such a scale is negligible compared with the variance corresponding to the sampling protocol, ς^2_{sam}, and the characterization method, ς^2_{cha}. This means that a finer scale of scrutiny is needed in order to study the influence of the grinding time on the pellet's homogeneity.

4. Investigation of the microstructural homogeneity of the green pellets

According to the results obtained in the previous section 3, another estimation of the homogeneity must be carried out at a much smaller scale in order to differentiate the grinding tests B01, B02 and B03.

Therefore, the microstructural homogeneity of the pellets obtained after co-grinding the powders have been investigated in this section.

4.1. SEM images

Three green pellets were prepared for each grinding or mixing conditions M01, B01, B02, B03 and B12. An example of some pellets prepared and being introduced into the SEM equipment is provided on Figure 5. The corresponding BSE images are shown on Figure 6. From these pictures, the grey level indicates the local composition: alumina appears in dark while zirconia corresponds to lighter areas. In order to compute the alumina fraction, the grey level images were turned into black and white ones, thanks to the Otsu method (Liu and Yu, 2009). Then, assuming that each pixel corresponds to at least one particle, the alumina fraction is obtained from the ratio between the number of black pixels and the total number of pixels of a given picture. The average alumina fractions, z_{BSE}, obtained for each grinding condition are given in Table 4. As it was already visible on Figure 6, the alumina content seems to decrease with the grinding time despite the fact that all ground powders have the same alumina mass fraction of $w = 0.3$.

Table 4 : Fraction of alumina observed on the BES-SEM pictures, z_{BSE}, as compared to the actual mass fraction of alumina w and to the corresponding surface fraction, z, of the pellets.

Test	z_{BSE}	w	z
M01	0.63 ± 0.01	0.30	0.60
B01	0.59 ± 0.01	0.30	0.54
B12	0.55 ± 0.00	0.30	0.42
B02	0.50 ± 0.01	0.30	0.44
B03	0.36 ± 0.01	0.30	0.46

First, it should be noticed that the measured alumina fraction, z_{BSE}, does not correspond to the alumina mass fraction of the entire pellet but rather represents a surface fraction at the top surface. This may explain why z_{BSE} decreases for longer grinding times. Indeed, the surface fraction of alumina within the blends depends on the fragmentation behavior of both powders during the ball milling step. The relationship between the alumina surface and the mass fractions of a binary mixture, containing alumina and zirconia powders, is given by equation (10).

$$z = \left[1 + \frac{d_{s,Al_2O_3}}{d_{s,ZrO_2}} \frac{\rho_{s,Al_2O_3}}{\rho_{s,ZrO_2}} \left(\frac{1}{w} - 1\right)\right]^{-1} \quad (10)$$

where $d_{s,i}$ is the average diameter of the surface particle size distribution of powder i and $\rho_{s,i}$ is its true density. This equation shows that the alumina surface fraction, z, depends on the ratio $d_{s,Al_2O_3}/d_{s,ZrO_2}$ which depends itself on the fragmentation behavior of each individual powder during the ball mill process.

The zirconia and the alumina powders were ground separately under the B01, B02, B12 and B03 conditions, in order to assess the effect of grinding on their particle size distribution. As a first approach, the B12 grinding conditions can be considered roughly equivalent to B02 in terms of energy provided to the particles, since the number of vessel revolutions is the same. The evolution of the volume and surface particle size distribution for each powder are shown on Figure 8. As expected, the particles are getting smaller according to the grinding time increase. In particular, the surface diameter of the zirconia particles significantly decreases after the ball milling operation as compared to that of the alumina powder. The surface fractions of alumina corresponding to a mass content of $w = 0.30$ were then computed for each grinding condition from equation (10), thanks to the mean surface diameter obtained

for both powders . It is important to keep in mind that we assumed that the fragmentation behavior of the powders during the ball milling operation was the same whether they are ground individually or in a co-grinding process. The results given in the last column of Table 4 show that the surface fraction of alumina is expected to decrease during the co-grinding process, which is consistent with the SEM images shown on Figure 6. Moreover, the comparison between the z_{BSE} and z values on Table 4 suggests that observed surface fraction, z_{BSE}, is representative for the actual surface fraction, z, of the co-ground powder mixture.

However, such results should be considered with care since many aspects are not taken into account in the calculation of z_{BSE}. Indeed, the methodology employed considers that all the pixels correspond either to an alumina or a zirconia particle, but the surface distributions presented on Figure 8 show that a large amount of particles of both powders have a diameter below 1.5 µm, which is the size of a given pixel on the SEM pictures. This becomes particularly critical after grinding. Moreover, the porosities, which represent around 50% in volume of the crude pellets, are not taken into account. Finally, we consider that the compaction of the powder may have a significant effect on the surface composition of the obtained images which has not been taken into account here. Indeed, the surface mean diameter of the powder blend does not necessarily corresponds to the average particle diameter observed at the surface of a compressed pellet.

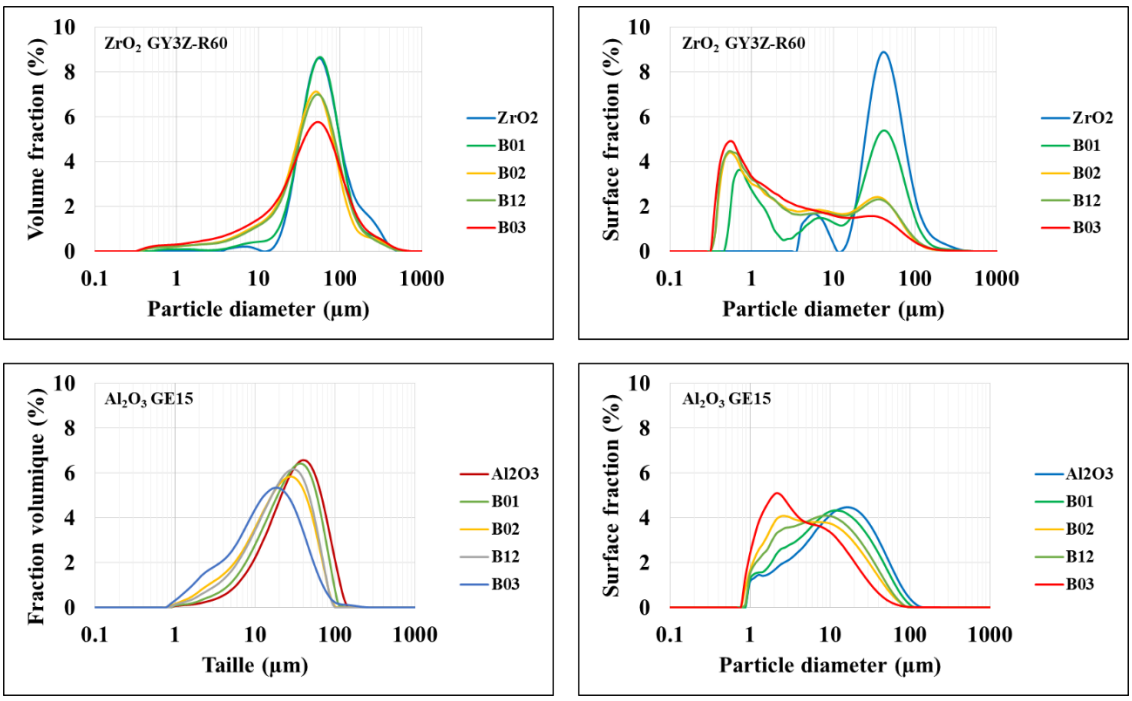

Figure 8: Evolution of the particle size distribution in volume (left) and in surface (right) according to the grinding conditions for the zirconia (up) and the alumina (down) powders.

Finally, in order to make sure that the composition z_{BSE} estimated from the method described above is related to the chemical composition of the areas shown on the pictures resumed on Figure 6, the same areas of interest were analyzed and quantified by EDS, focusing on the Al and Zr elements. Then, for each pixel of the map, the aluminum content was calculated. The measured compositions, z_{EDS}, are compared to the ones obtained by BSE, z_{BSE}, on Figure 9. On this figure, the crosses represent the data obtained from SEM areas taken at a higher magnification of x250. This complementary analysis was carried out in order to consolidate the results and to make sure that there is no bias introduced by the low resolution of the x80 SEM images. The resolution being 1.5 μm per pixels for the x80 images and 0.6 μm per pixel for the x250 ones, most of the particles are bigger than one pixel on the x250 images, according to the particle size distributions given on Figure 8.

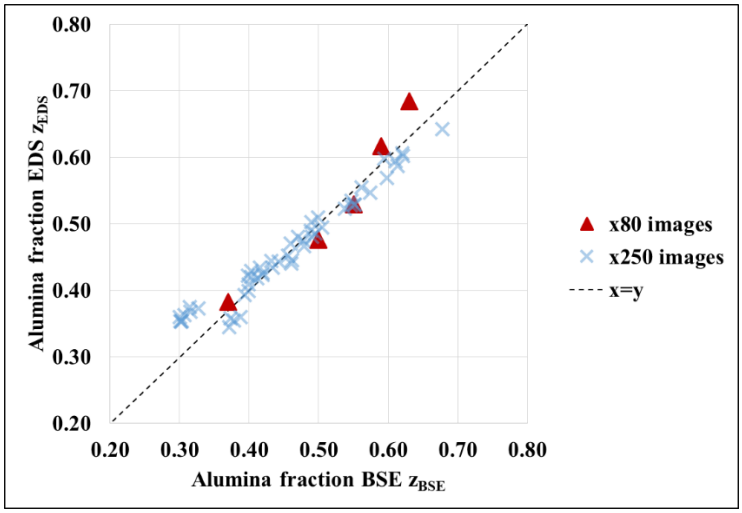

Figure 9: Comparison between the alumina fraction measured at the surface of a pellet with BSE and EDX analysis. Images were captured at magnifications of x80 and x250 for each grinding condition

Figure 9 clearly shows that the alumina content from the areas considered and estimated from EDS or BSE approaches are very similar, whatever the surface composition of the pellet. Furthermore, it seems that there is no effect of the low resolution of the x80 SEM images on the obtained results. Therefore, the microstructure of the pellets can be investigated from the BSE images shown on Figure 6.

a mis en

a suppri

a suppri

4.2. Multi-scale analysis of area fractions

In this section, random black and white images were generated in order to check the consistency of the methodology. An example of an image generated with a Matlab® program, developed by (Tschopp et al., 2008), is given on Figure 10. In this example, the surface fraction of black pixels was set to $z = 0.15$, the black ellipsoidal particles' size, location and orientation are randomly generated.

a suppri

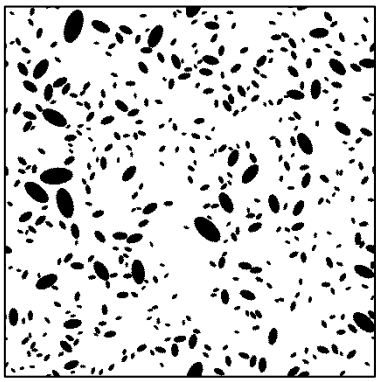

Figure 10: Example of binary microstructure randomly generated on Matlab®

The multi-scale analysis of area fraction (MSAAF) methodology consists in replacing a group of adjacent pixels, also called a cell, by one pixel representing the average value of the whole cell. An example applied to Figure 10 is presented on Figure 11, where the cell size, denoted as Q, can vary from 1 pixel (only one pixel for the whole image) to $L = 1024$ pixels. For each configurations represented on Figure 11, the intensity of segregation associated to the scale of scrutiny Q can be assessed by calculating the coefficient of variation between the cells value. The evolution of the coefficient of variation associated to the microstructure shown on Figure 10 as a function of the scale of scrutiny has been represented on the right side of Figure 11.

a suppri

a suppri

a suppri

a suppri

a suppri

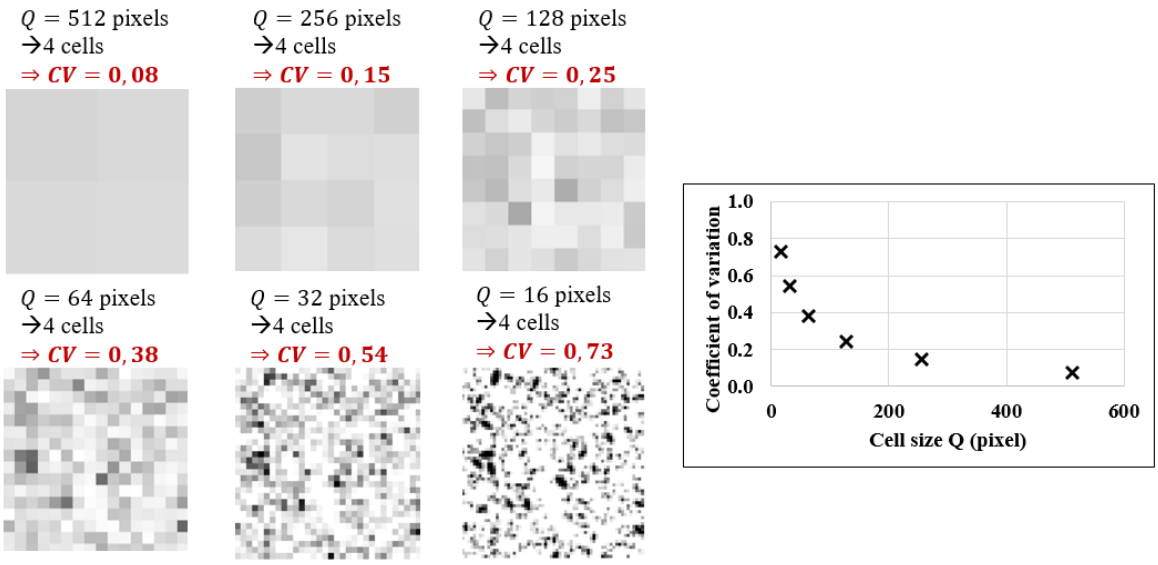

Figure 11: Example of application of the MSAAF methodology applied to the microstructure represented on Figure 10

a suppri

It appears that it is possible to define the maximal cell size providing a given coefficient of variation. For example, if the acceptability criteria is set to $CV = 6\%$, as in the pharmaceutical industry, this methodology gives the scale at which the microstructure can be considered as homogeneous. This scale corresponds to the scale of segregation. In such a method, it is more convenient to express the scale of scrutiny by the dimensionless ratio λ represented by equation (11), instead of using the cell size Q, as in Figure 11.

a suppri

$$\lambda = \frac{Q}{\bar{d}} \tag{11}$$

where $\bar{d}$ is the average particle size on the images.

If the cell size becomes significantly lower than the mean particle size ($\lambda \ll 1$), then the measured variance will approach the maximal variance possible of a completely segregated mixture, ς_0^2, given by equation (12) (Lacey, 1954).

$$\varsigma_0^2 = z_{BSE} \cdot (1 - z_{BSE}) \tag{12}$$

where z_{BSE} is the surface fraction observed on the image. The corresponding coefficient of variation is expressed by:

$$CV_0 = \frac{\varsigma_0}{z_{BSE}} = \sqrt{\frac{1 - z_{BSE}}{z_{BSE}}} \tag{13}$$

In this case, the coefficient of variation measured for this scale does not reflect the microstructure of the image but mostly depends on its composition. Therefore, we must ensure that the scale λ is higher than 1, so that the coefficient of variation is a characteristic parameter describing the microstructural homogeneity.

4.3. Comparison of the grinding conditions in terms of microstructure of the green pellets

The SEM pictures obtained on the different green pellets made from various grinding conditions can be compared in terms of microstructural homogeneity by employing the MSAAF method described just above. Before applying this method, the mean particle size $\bar{d}$ observed on each picture must be defined, in order to be able to express the scale λ. This was done by measuring the mean particle diameter

observed on each SEM picture. 25 particles diameters were measured per pellets with the ImageJ® (NIH, Bethesda, USA) software. Since three pellets were prepared per grinding conditions, this means that the average particle diameters were computed from 75 measurements. The values of $\bar{d}$ taken for each grinding condition are summarized in Table 5. The MSAAF measurements are represented on Figure 12. A focus on the MSAAF corresponding to the B01 grinding condition alone is shown on Figure 13.

a suppri

a suppri

a suppri

It appears that the measured data, represented by crosses on these figures, are consistent with the asymptotical behaviors represented by the dotted lines. Indeed, the measured coefficients of variation seem to approach the theoretical maximal value of C_0, given by equation (13), as the cell size becomes lower than the particle mean diameters ($\lambda < 1$). As λ becomes higher, the MSAAF curves seem to decrease linearly (on a log-log scale). In a similar study, Spowart suggested the Poisson law for describing the asymptotical behavior of the MSAAF curve for $\gg 1$ (Spowart et al., 2001). However, in our case, SEM picture at much larger scales would be needed in our case in order to study in more details the behavior of the coefficient of variation at higher λ.

It is also interesting to note that the MSAAF curves are located lower on the graph as the grinding time increases. Indeed, for a given scale λ, the M01 pellets exhibit the highest coefficient of variation, while the B03 ones exhibit the lowest. Concerning the B02 and B12 tests, they present similar MSAAF curves, this was expected since they both correspond to similar energetic conditions (100 vessel's revolutions) for grinding.

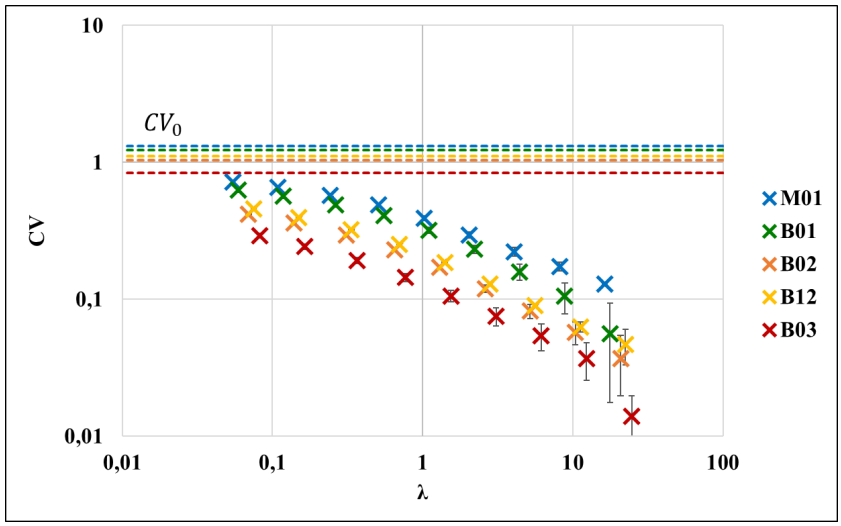

Figure 12: MSAAF analysis presented for various grinding conditions, the error bars represent the standard deviations between three pellets of the same grinding test

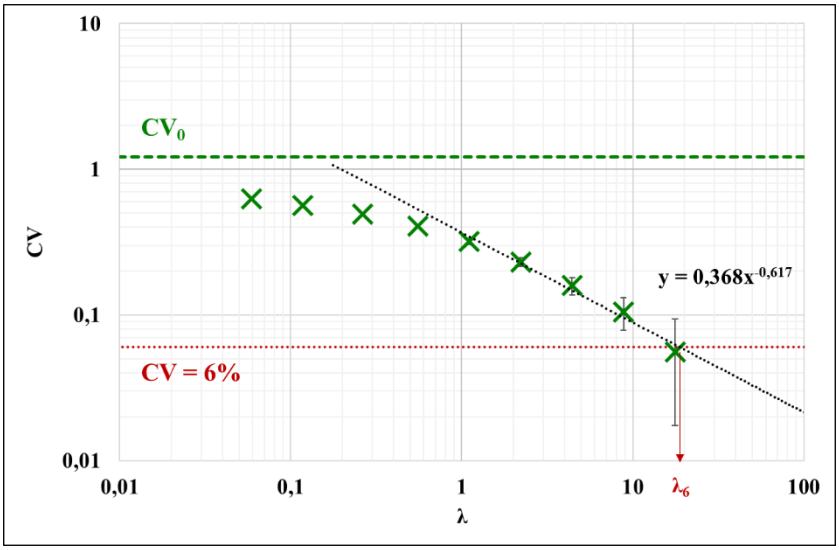

Figure 13: MSAAF obtained for the B01 grinding test

The scale of acceptability λ_6, at which a coefficient of variation of 6% is reached, can be deduced from the MSAAF data presented on Figure 12, for each grinding condition. The specific value of 6% was chosen because it is the most common criteria used in the pharmaceutical industry. However, any other criteria can be chosen instead, without modifying the methodology. The value of λ_6 can be estimated by extrapolating the measured data with a power law fit. Since the MSAAF curves exhibit two asymptotical behaviors, the power law fit was computed for the values corresponding to $\lambda > 1$ only, as represented on Figure 13. This means that the limit of acceptability should be chosen accordingly with the range of the λ values observed. As an example, a coefficient of variation of 1% is never reached for the range of λ investigated, which means that the extrapolation is highly uncertain. The obtained values of λ_6 for each grinding condition are summarized in Table 5. Then, the corresponding cell size, Q_6, can be computed from the particles' diameters measured previously, the results being also resumed in Table 5.

a suppri

a suppri

a suppri

a suppri

Table 5: Scale of acceptability corresponding to a coefficient of variation of 6% for each grinding condition

Test	$\bar{d}$ (μm)	λ_6	Q_6 (µm)	W_6 (µg)	H_6
M01	40.2 ± 2.6	112	4515	~ 1 300	2.6
B01	37.1 ± 3.1	19	701	~ 50	4.0
B12	31.5 ± 1.4	13	378	~ 7	4.9
B02	29.2 ± 2.2	9	285	~ 5	5.0
B03	26.6 ± 0.3	5	127	~ 0.5	5.9

Table 5 shows that the scale of scrutiny needed to get a coefficient of variation of 6% decreases with the grinding time. This means that co-grinding the powders allows an homogenization of the powders at a finer scale. For example, a square cell of 127 μm, taken randomly at the surface of a pellet prepared with powders ground in the B03 conditions, can be considered as representative of the overall surface composition of the pellet with a margin of error of 6%.

a suppri

The obtained scales of acceptability, Q_6, correspond to the lengths of squared cells observed at the surface of the pellets. In order to be able to compare these results to the macroscopic scale investigated in section 3, they can be converted into sample mass from equation (14).

$$W_6 = \rho_{pellet} \times {Q_{6\%}}^2 \times q \qquad (14)$$

where ρ_{pellet} is the apparent density of a given pellet whose dimensions were measured with a caliper and q represents the depth over which the composition can be considered equal to the measured surface composition. For this approximate calculations, we considered a value of $q = 20\ \mu m$, which roughly corresponds to the diameter of a given particle. The results are given on Table 5. Although these values are only approximations, they are significantly lower than the macro and intermediate scales investigated before in this paper.

Finally, the homogeneity index H_6 proposed by Buslik can be computed from equation (3), the results are summarized in the last column of Table 5. This index gives an indicator about the evolution of the homogeneity according to the grinding time. It appears clearly that the microstructural homogeneity is significantly improved by the co-grinding process, as compared to a single drum mixing procedure represented by the M01 test and that the homogeneity keeps improving during the first minutes of grinding.

Concerning the B02 and B12 co-grinding tests, it seems that B02 conditions provide a slightly better homogeneity index than the one obtained for the B12 conditions. This means that the B02 test is better mixed in terms of microstructure despite the fact that the number of vessel revolution are the same (2 minutes at 50 rpm for B12 and 4 minutes at 25 rpm for B02). These results suggest that the number of revolution may not be the most relevant parameter that governs the microstructural homogeneity of the pellets. The evolution of the computed scales of acceptability, Q_6, according to the grinding time is represented on Figure 14. It appears that the data can be interpolated using a power law, represented by the dotted line. This suggests that the microstructure of the pellets made from co-ground powders seem to depend mainly on the grinding time rather than on the number of vessel's revolutions. It should be noted that this is only valid for the range of rotational speed investigated (25 and 50 rpm), which both correspond to the same rolling regime of the pebbles within the rotating vessel. Figure 14 also suggests that the microstructural homogeneity is improved significantly during the first minutes of grinding and becomes almost stable beyond 2 minutes.

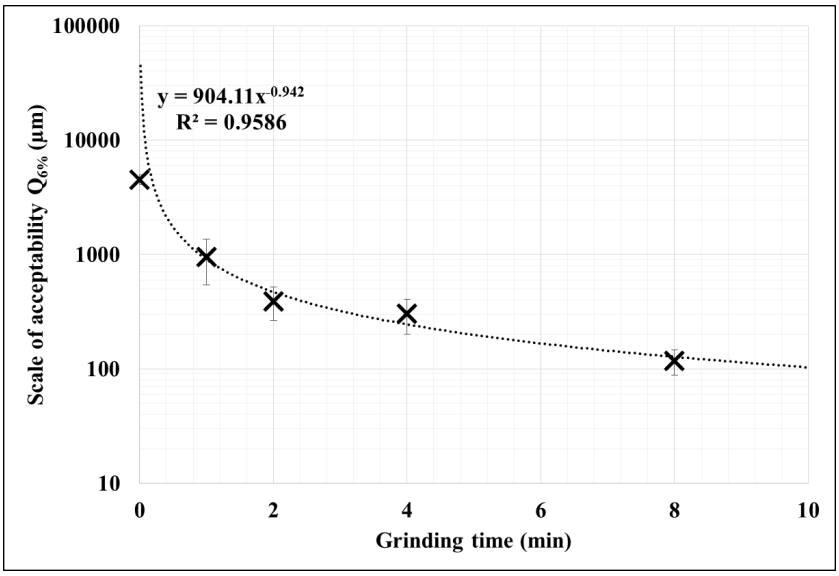

Figure 14: Evolution of the scale of acceptability, $Q_{6\%}$, of the crude pellets, according to the grinding time

5. Conclusions and perspectives

In this paper, various co-grinding conditions were compared in terms of resulting homogeneity at different scales. In section 3, we showed that the mixing of powders operated in a ball mill allows an improvement in terms of macro-homogeneity as compared to the use of a simple drum mixer. Indeed, the co-grinding process systematically gives pellets of 1 g of the same composition with a margin of error below 2%. However, no difference was observed between the grinding tests at such a macroscopic

scale, which makes it impossible to investigate the effect of the grinding time on the homogeneity of resulting ground powder. This can be interpreted in two main ways :

- The most homogeneous mixture theoretically achievable at such a scale is obtained after only one minute of grinding,
- or the evolution of the homogeneity at this scale becomes negligible as compared to the variance associated to the sampling procedure or to the characterization method.

For both interpretations, this means that the variance observed at this scale of 1 g is not the most relevant for describing the homogeneity of the co-ground powders.

The methodology employed for estimating the homogeneity in this section 3 is the standard approach, based on Dankwert's definitions of the scale and intensity of segregation. Such method is described schematically on Figure 15, and relies on the scale of scrutiny considered, which has to be defined at first. Then, the sampling procedure and the characterization method are defined in order to estimate the homogeneity from the variance observed. In this paper, this method failed to differentiate the grinding conditions in terms of homogeneity. Indeed, the measured variance did not seem to vary according to the grinding time. This shows the limitations of such standard methodology described by the continuous arrows on Figure 15. Indeed, the homogeneity measured by this approach only makes sense if the scale of scrutiny is adequate, but not only such scale is rarely known in advance but it is susceptible to vary according to the operating conditions. In the particular case of powder mixtures prepared by co-grinding, the scale of scrutiny varies with the particle size, which is expected to decrease according to the grinding time.

The grinding tests were finally compared by investigating the microstructure of green pellets obtained by compacting the co-ground powders. A reverse method, based on the MSAAF analysis, was developed and is schematized by the dotted lines on Figure 15. Such method provides a homogeneity index, H_6, associated to the scale, W_6, at which the pellets can be considered as acceptable in terms of homogeneity. The scale W_6, measured from SEM images is closely related to the actual scale of segregation of the mixture as defines by Dankwerts (Danckwerts, 1953).

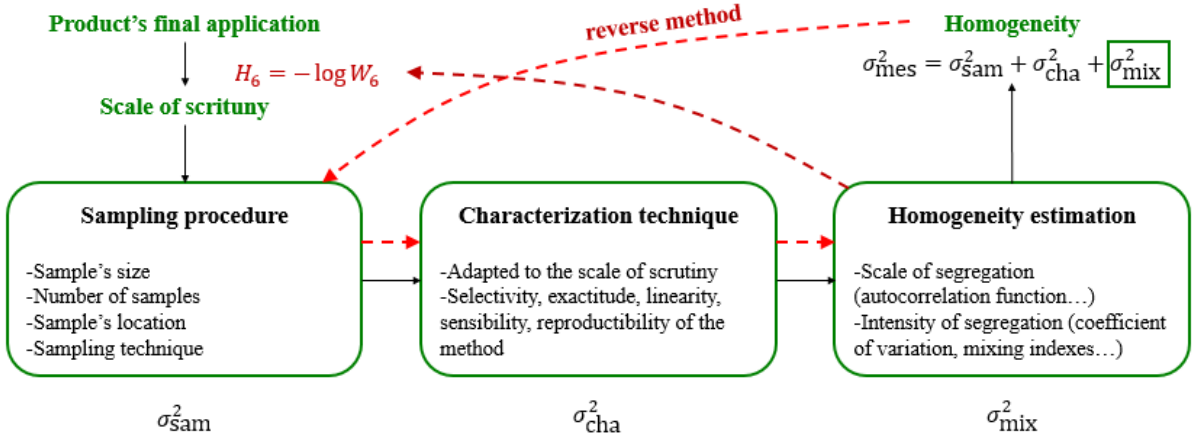

Figure 15: Schematic representation of the standard methodology leading to the estimation of the homogeneity of a given powder mixture, and the reverse method developed in this paper.

This time, a clear variation was observed between the different co-grinding conditions investigated. It appeared that the scale of acceptability, corresponding to a coefficient of variation of 6%, evolved almost inversely with the grinding time. This mean that the co-grinding process allows a better microstructural homogenization, in particular during the first minutes of grinding.

Now that the scale of acceptability, W_6, has been estimated, a deeper analysis can be carried out by investigating more precisely the homogeneity at the relevant scale of scrutiny. For example, for the B02 co-grinding condition, whose scale of acceptability was estimated at around $300\ \mu m$, the homogeneity can be estimated in more details from SEM pictures taken at a magnification around x400, which approximately corresponds to an image dimension of $300\ \mu m$ with a much better resolution than the one obtained at x80. The optimal number of x400 SEM picture needed to estimate correctly the homogeneity can be obtained from the t-Student or the χ^2 laws, knowing that the coefficient of variation at such scale is near 6% (Massol-Chaudeur, 2000). Then, the standard procedure, shown on Figure 15, can be estimated from such images. This complementary analysis, in addition to be more precise thanks to the finer resolution of the images, may also include an estimation of the scale of segregation by studying the autocorrelation function of the pellets at this scale, as done previously by Mayer-Laigle (Mayer-Laigle et al., 2011). Thus the methodology described in this paper, and more precisely in section 4, can be seen as a preliminary analysis providing the most relevant scale for investigating the microstructural analysis.

a suppri

For future works, it would be of a great interest to investigate the relation found between the scale of acceptability and the co-grinding time into more details. In particular, the obtained results could be compared to mixing kinetics models. Grinding kinetics models could also be used to predict the evolution of the particle size distribution according to the grinding time. This may provide meaningful information concerning the particle size and the scale of acceptability at a given composition.

List of figures:

List of tables:

Bibliography

Bergum, J.S., Prescott, J.K., Tejwani, R.W., Garcia, T.P., Clark, J., Brown, W., 2014. Current events in blend and content uniformity. Pharm. Eng., Product development 34, 28–39.

Berthiaux, H., 2002. Mélange et homogénéisation des solides divisés. Tech. Ing. Mise En Forme Médicam. base documentaire : TIB611DUO.

Buslik, D., 1973. A proposed universal homogeneity and mixing index. Powder Technol. 7, 111–116. https://doi.org/10.1016/0032-5910(73)80014-2

Danckwerts, P., 1953. Theory of mixtures and mixing. Research 6, 355–361.

Danckwerts, P.V., 1952. The definition and measurement of some characteristics of mixtures. Appl. Sci. Res. Sect. A 3, 279–296. https://doi.org/10.1007/BF03184936

FDA, 2003. Powder Blends and Finished DosageUnits — Stratified In-Process DosageUnit Sampling and Assessment, Guidance for industry. U.S. Department of health and Human Services food and drug administration.

Giraud, M., Gatumel, C., Vaudez, S., Bernard-Granger, G., Nos, J., Gervais, T., Berthiaux, H., 2020. Investigation of a granular Bond number based rheologican model for polydispersed particulate systems. Press.

Harnby, N., 1992. Chapter 2 - Characterization of powder mixtures, in: Harnby, N., Edwards, M.F., Nienow, A.W. (Eds.), Mixing in the Process Industries. Butterworth-Heinemann, Oxford, pp. 25–41. https://doi.org/10.1016/B978-075063760-2/50023-8

Lacey, P.M.C., 1954. Developments in the theory of particle mixing. J. Appl. Chem. 4, 257–268. https://doi.org/10.1002/jctb.5010040504

Liu, D., Yu, J., 2009. Otsu Method and K-means, in: 2009 Ninth International Conference on Hybrid Intelligent Systems. Presented at the 2009 Ninth International Conference on Hybrid Intelligent Systems, pp. 344–349. https://doi.org/10.1109/HIS.2009.74

Massol-Chaudeur, S., 2000. Caractérisation de l'état de mélange de poudres : cas de mélanges faiblement dosés.

Mayer-Laigle, C., Gatumel, C., Berthiaux, H., 2015. Mixing dynamics for easy flowing powders in a lab scale Turbula® mixer. Chem. Eng. Res. Des. 95, 248–261. https://doi.org/10.1016/j.cherd.2014.11.003

Mayer-Laigle, C., Gatumel, C., Berthiaux, H., 2011. A 2D autocorrelation method for assessing mixture homogeneity as applied to bipolar plates in fuel cell technology. Adv. Powder Technol. 22, 167–173. https://doi.org/10.1016/j.apt.2010.09.005

Poux, M., Fayolle, P., Bertrand, J., Bridoux, D., Bousquet, J., 1991. Powder mixing: Some practical rules applied to agitated systems. Powder Technol. 68, 213–234. https://doi.org/10.1016/0032-5910(91)80047-M

Schofield, C., 1976. The definition and assessment of mixture quality in mixtures of particulate solids. Powder Technol. 15, 169–180. https://doi.org/10.1016/0032-5910(76)80045-9

Spowart, J.E., Maruyama, B., Miracle, D.B., 2001. Multi-scale characterization of spatially heterogeneous systems: implications for discontinuously reinforced metal–matrix composite microstructures. Mater. Sci. Eng. A 307, 51–66. https://doi.org/10.1016/S0921-5093(00)01962-6

Tschopp, M.A., Wilks, G.B., Spowart, J.E., 2008. Multi-scale characterization of orthotropic microstructures. Model. Simul. Mater. Sci. Eng. 16, 065009. https://doi.org/10.1088/0965-0393/16/6/065009